
An effective analytical model for springback prediction in straight flanging processes

Thaweepat Buranathiti and Jian Cao*

Mechanical Engineering, Northwestern University, Evanston, IL, USA

E-mail: jcao@northwestern.edu

*Corresponding author

Abstract: In many manufacturing processes involving sheet metal fabrications, springback is a major concern, complicating tooling designs. This paper develops an effective analytical model to predict springback for a straight flanging process. The model calculates the final springback angle by conducting bending moment computation, geometry and configuration calculation, and springback calculation. The predicted results are examined against our own experimental data and experimental results from independent papers. The predicted results show a good agreement with the corresponding experimental results published in the literature. Sensitivity and trend analysis of springback are efficiently obtained.

Keywords: analytical model; sheet metal forming process; springback; straight flanging process.

Reference to this paper should be made as follows: Buranathiti, T. and Cao, J. (2004) 'An effective analytical model for springback prediction in straight flanging processes', *Int. J. Materials and Product Technology*, Vol. 21, Nos. 1/2/3, pp.137–153.

Biographical notes: Thaweepat Buranathiti is currently a Graduate Student in Mechanical Engineering at Northwestern University. He received his BEng degree in Aerospace Engineering and his MEng degree in Industrial Engineering from Kasetsart University, Bangkok, Thailand.

Prof. Jian Cao is an Associate Professor at Northwestern University. She received both her BS degrees in Materials Engineering and Automotive Control from Shanghai JiaoTong University of China, and her MSc and PhD degrees in Mechanical Engineering from M.I.T. Prof. Cao's primary technical interests are in the mechanics analysis and design of macro/micro metal forming and composite sheet forming processes. She is an Associate Editor for *ASME Journal of Manufacturing Science and Engineering*, <http://www.mech.northwestern.edu/fac/cao>.

1 Introduction

In every industry, quality and productivity are major issues for being competitive. For example, a car frame needs to be designed to achieve strength requirements and aesthetic aspects; on the other hand, cost of production and repeatability is crucial to

the business. A stamping process has been one solution used in practice to achieve these goals in the sheet metal fabrication business. However, springback, a shape discrepancy between the fully loaded and unloaded configurations, undermines the stamping benefits, since a major effort on the tooling design is needed to compensate springback. In many industries, e.g. automotive industries, springback plays an important role in tooling and process designs. Two main branches of springback research have been conducted: to effectively predict springback; and to compensate for springback in tooling design. This paper aims at the first branch for a simple straight flanging process, which is a case of either creating a mating surface to other parts or increasing the stiffness of this particular part.

To effectively predict springback for a potential application in determining optimal tooling shapes and process parameters, understanding the mechanics of springback, a mainly elastic recovery process, is essential. Experimental studies [1–7] in bending/flanging of a straight flanging process mainly involve: gap; die corner radius; material type (e.g. steel, aluminium, etc.); and binder force, as the main parameters. It is generally found that springback decreases as the die corner radius decreases, the gap to thickness ratio decreases, the binder force increases, and the punch nose radius decreases. However, the punch nose radius has an influence on springback within a relatively narrow range, i.e. it has less influence at a larger nose radius [3].

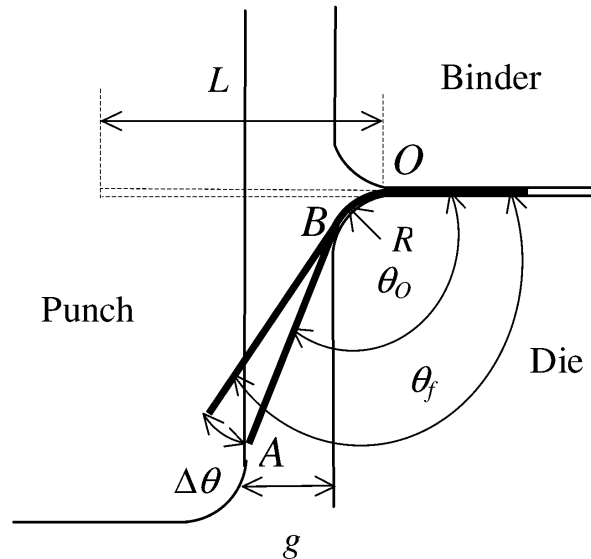
This paper develops an analytical springback prediction model for a straight flanging process and presents the effectiveness by comparing with results published in References [6–8] and is conducted at the Advance Materials Processing Laboratory (AMPL) at Northwestern University. The rest of this paper is organised as follows: the details of the straight flanging process are studied in Section 2, the proposed analytical model in Section 3, the comparison in Section 4, and, finally, the summary and concluding remarks in Section 5. The appendix, explaining some derivations, is presented at the end of the paper.

2 Process definition

This paper uses a straight flanging process to develop a model for springback prediction to sheet metals with a number of different tooling set-ups and materials. The effectiveness of the model is verified with a comparison between the predicted results and the corresponding experiments.

2.1 *A straight flanging process and springback*

A flanging process basically consists of a punch, a binder, a die, and a blank. In this paper, the process is mainly characterised by the gap and the die corner radius. The tooling set-up is shown in Figure 1 with the following characteristics: the die root position O , the separation point B between the deformed sheet and the die, the touching point A between the deformed sheet and the punch, the flange length L , and the gap g between the die and the punch. The fully loaded configuration is represented by θ_0 , and the fully unloaded configuration is described by θ_f . The springback angle is defined by $\Delta\theta = \theta_f - \theta_0$.

Figure 1 Schematic of a straight flanging process

2.2 Experiments

The dimension of the sheet blank used in the flanging experiments is 203.2×203.2 mm (or 8×8 in). The experiments are performed by a 150-ton computer controlled HPM hydraulic press at the Advance Materials Processing Laboratory (AMPL) at Northwestern. The fully unloaded configuration θ_f is measured by using a coordinate measuring machine (CMM: Brown & Sharpe MicroVal Series B89) at the metrology laboratory at Northwestern. A number of tests at each tooling set-up have been conducted in order to observe the possible variation. In addition, experimental data published in References [6–8] are used to validate the proposed analytical model. It should be noticed that these papers have only a single result for each tooling set-up by neglecting uncertainty concerns.

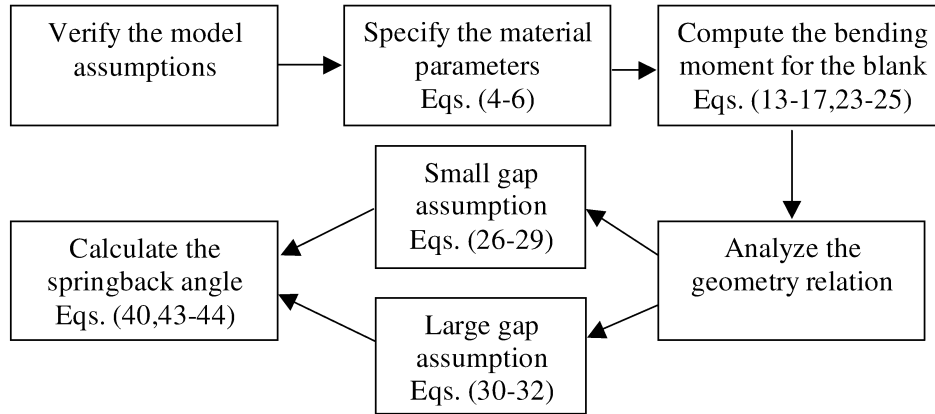
3 Analytical model

In an early design stage, a quick estimation is essential and beneficial to the entire design process. In this paper, an analytical model for springback prediction in a straight flanging process is proposed and based on an earlier model in [2]. In [2], the model assumes a linear moment distribution from point B and point O with $M' = \frac{M_O}{M_B}$. M' was obtained by fitting sample cases studied using finite element methods. This can be reduced to Wang's model [6] by setting $M' = 0$. Here, M' is explicitly derived and calculated. Additionally, the model is proposed for an arbitrary flanging angle rather than only a 90° flanging angle, as in [2]. As most of the analytical models, the following assumptions are used in our analytical model:

- the sheet metal is in plane strain conditions along the flange width direction and in plane stress conditions along the sheet thickness direction
- the sheet metal is homogeneous and isotropic
- the sheet metal follows the power hardening law and von Mises' yield criterion
- planes normal to the sheet surface remain planes during the deformation process
- Bauschinger effect is neglected
- the middle layer of the sheet is considered to be bending-strain-free
- volume conservation is assumed so that the volume variation due to elastic deformation is negligible
- moment distributions along the straight and curved parts are linear (discussed in [1])
- only elastic deformation occurs in the unloading stage.

The main elements in constructing the analytical model are: the definition of strain and stress expressions for the deformed sheet; the computation of bending moment in the sheet under the fully-loaded configuration; the analysis of geometry associated with the tooling set-up; and the springback calculation resulted by releasing the stored bending moment to the pure elastic unloading. The flow chart is shown in Figure 2.

Figure 2 The flow chart for the analytical model



3.1 Strain and stress expressions

Define the curvature κ of the deformed sheet with thickness t as

$$\kappa = \frac{1}{R_d + t/2} = \frac{1}{R}, \quad (1)$$

where R_d is the die corner radius and R is the effective bending radius. The expression

of the true strain (ε) for the deformed sheet is derived in the Appendix and summarised in

$$\varepsilon = \kappa\zeta, \quad (2)$$

where the local coordinate $\zeta \in \left[-\frac{t}{2}, \frac{t}{2}\right]$. At a large value of $\kappa\zeta$, the above true strain expression mathematically requires additional terms as later discussed in Section 4. The true stress (σ) follows the power hardening law with the strength coefficient as K and the exponent coefficient as n

$$\sigma = K\varepsilon^n. \quad (3)$$

The material parameters obtained from uniaxial tensile tests under the plane stress conditions (Young's modulus E and yield stress Y) need to be modified for the model under the plane strain conditions [9, p.79, 10–11]. Using von Mises law, the new E' and Y' for plane strain calculation are

$$E' = \frac{E}{1 - \nu^2}, \quad (4)$$

$$Y' = \frac{2Y}{\sqrt{3}}, \quad (5)$$

where ν is the Poisson ratio. In addition, the parameter K for the plastic region needs to be adjusted by using the same von Mises law as

$$K' = \frac{2K}{\sqrt{3}}. \quad (6)$$

The parameter n remains the same. Note that for simplicity, E' , Y' , and K' are later written in E , Y , and K . Due to the existence of the Luders band in many materials as shown in Figure 3, we define the yield strain ε_{y1} corresponding to Y from the Hooke's law, the fibre position t_{y1} corresponding to ε_{y1} , the yield strain ε_{y2} corresponding to Y obtained from the power law, the fibre position t_{y2} corresponding to ε_{y2} , and the bending moment M_y of the elastic limit of the sheet or the bending moment where yielding occurs on the sheet surface as:

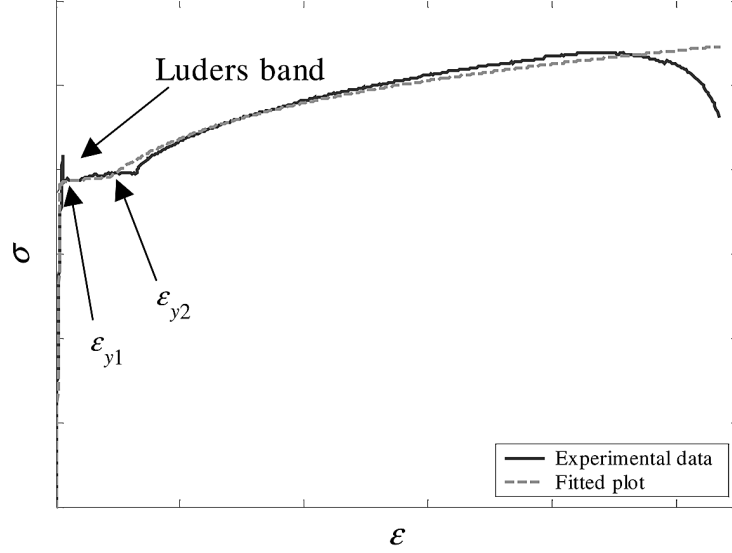
$$\varepsilon_{y1} = \frac{Y}{E}, \quad (7)$$

$$t_{y1} = \frac{\varepsilon_{y1}}{\kappa}, \quad (8)$$

$$\varepsilon_{y2} = \text{MAX} \left[\varepsilon_{y1}, \left(\frac{Y}{K} \right)^{\frac{1}{n}} \right], \quad (9)$$

$$t_{y2} = \frac{\varepsilon_{y2}}{\kappa}, \text{ and} \quad (10)$$

$$M_y = \frac{2}{3} Y \left(\frac{t}{2} \right)^2. \quad (11)$$

Figure 3 A stress–strain diagram with the present of the Luders band

3.2 Bending moment computations

Bending moment (M) of the deformed sheet is defined as

$$M = \int_{-t/2}^{t/2} \zeta \cdot \sigma(\zeta) d\zeta. \quad (12)$$

For simplicity of the model, the bending moment of the deformed sheet is decomposed into the bending moment M_{elas} associated with the elastic region, the bending moment M_{plas1} associated with the Luders band, and the bending moment M_{plas2} associated with the plastic region under the power law as follows

$$M_{elas} = \frac{2}{3} E \cdot \kappa \cdot (t_{y1})^3, \quad (13)$$

$$M_{plas1} = \text{MIN} \left[Y \cdot \left(\left(\frac{t}{2} \right)^2 - (t_{y1})^2 \right), \text{MAX} \left\{ Y \cdot \left((t_{y2})^2 - (t_{y1})^2 \right), 0 \right\} \right], \quad (14)$$

$$M_{plas2} = \text{MAX} \left[\frac{1}{2} \frac{K \cdot t^2 (\kappa \cdot t)^n}{(n+2)2^n} - \frac{2K \cdot t_{y2}^2 (\kappa \cdot t_{y2})^n}{(n+2)}, 0 \right], \quad (15)$$

and it can be simplified as

$$M_{plas2} = \text{MAX} \left[\frac{K}{n+2} \frac{2}{R^n} \left(\left(\frac{t}{2} \right)^{n+2} - t_{y2}^{n+2} \right), 0 \right], \quad (16)$$

$$M_{elasplas} = M_{elas} + M_{plas1} + M_{plas2}, \quad (17)$$

where $M_{elasplas}$ is the total bending moment of one section of the sheet with respect to a certain bending curvature. Note that ‘MAX’ and ‘MIN’ operators in Equations (14)–(16) are in cases that $\frac{t}{2} < t_{y1}$ or $\frac{t}{2} < t_{y2}$.

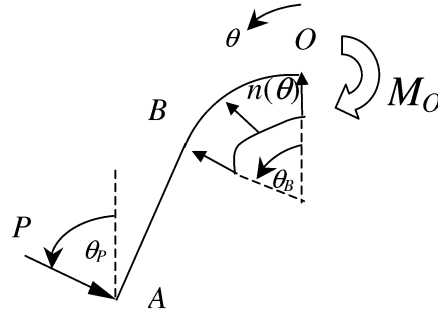
Considering a free body diagram in Figure 4, the bending moment M_O at the die root O and the normal pressure $n(\theta)$ along the curved part between B and O , $\theta \in [0, \theta_B]$, are the external forces from the flanging. The bending moment M_B at B is approximately equal to the calculated bending moment $M_{elasplas}$ as

$$M_B = M_{elasplas}. \quad (18)$$

The force P acting normally at A with the angle θ_P with respect to the vertical direction is the external force from the punch for being sheet in contact with. Having the distance between A and B being l , P is approximately as

$$P = \frac{M_B}{l}. \quad (19)$$

Figure 4 A free body diagram of the flanged sheet



Using the arbitrarily distributed pressure $n(\theta)$ along the curved part S between B and O , we derived the bending moment M_O from the equilibrium conditions as

$$\sum F_x = 0, \quad (20)$$

$$\sum F_y = 0, \text{ and} \quad (21)$$

$$\sum M = 0. \quad (22)$$

From Equation (20), the equilibrium equation on the x -direction is written as

$$P \sin \theta_P = \int_S n(\theta) \sin \theta ds = R \int_{\Theta} n(\theta) \sin \theta d\theta.$$

Similarly, from Equation (21), the equilibrium equation on the y -direction is written as

$$P \cos \theta_P = \int_S n(\theta) \cos \theta ds = R \int_{\Theta} n(\theta) \cos \theta d\theta.$$

From Equation (22), the moment equilibrium equation around the point O is written as

$$M_O = P \cos(\theta_P - \theta_B)(l + R \sin \theta_B) - P \sin(\theta_P - \theta_B)R(1 - \cos \theta_B) - \int_S R \cdot n(\theta) \sin \theta ds.$$

Therefore, an expression for the bending moment M_O is written as follows

$$M_O = P[\cos(\theta_P - \theta_B)(l + R \sin \theta_B) - R \sin(\theta_P - \theta_B)(1 - \cos \theta_B) - R \sin \theta_P],$$

and can be simplified as

$$M_O = P[l \cos(\theta_B - \theta_P) + R \sin(\theta_B - \theta_P)]. \quad (23)$$

Two non-dimensional parameters, i.e. M' and γ_B , are proposed to simplify the expressions and to characterise the process as follows

$$M' = \frac{M_O}{M_B}, \text{ and} \quad (24)$$

$$\gamma_B = \frac{M_B}{M_y}. \quad (25)$$

3.3 Geometry analysis for the fully loaded configuration (before springback)

The parameters (l , θ_B , θ_P , and S) used in the force/moment expressions are calculated from the geometry relations. We divide the calculation into two cases, i.e. a small gap and a large gap. A set of explicit expressions can be obtained for the small gap assumption while a set of nonlinear system equations needs to be solved for the large gap assumption.

For a small gap ($g/t < 2$), a set of geometry parameters in Figure 1 was derived in [2] and adopted here as follows

$$l \approx \sqrt{\frac{R(g-t)}{\eta_0 - \psi_0}}, \quad (26)$$

$$\theta_B = \theta_P - \theta_l, \text{ and} \quad (27)$$

$$S = R\theta_B, \quad (28)$$

where

$$\begin{aligned} \eta_0 &= \frac{n}{n+1} + \frac{(n+2)(1-n)}{2(n+1)} \varphi_0^{n+1}, \\ \psi_0 &= \frac{n}{2n+1} + \left(\frac{1+8n^2}{3(1+3n+2n^2)} + \frac{1-2n}{1+n} + \frac{1}{3} \right) \varphi_0^{2n+1} \left(\frac{n+2}{3} \right)^2, \\ \varphi_0 &= \frac{\varepsilon_y}{\varepsilon(\zeta=t/2)} = \frac{Y R}{E t/2}, \\ \theta_P &\approx \frac{\pi}{2}. \end{aligned} \quad (29)$$

Note that by calculating θ_l in the springback calculation section, θ_B is obtained.

For a large gap, the parameters (l and θ_B) are calculated from solving the following two equations:

$$w \sin \theta_B + \left(g - \frac{t}{2}\right) + \left(R - \frac{t}{2}\right) = l \cos \theta_B + R \sin \theta_B, \quad (30)$$

$$\tan\left(\frac{\pi}{2} - \theta_B\right) \approx \frac{12}{E \cdot t^3} \left(\frac{M_B l}{2}\right), \quad (31)$$

where

$$w \approx \frac{l^2}{\gamma_B^2} \frac{2\varepsilon_{y1}}{t}. \quad (32)$$

Then we used Equations (27)–(28) to obtain θ_p and S . Equation (31) is used to approximate the deflected angle by assuming a classical bending theory. To solve this nonlinear system equation [Equations (30)–(32)], a nonlinear solving method (e.g. Newton–Raphson method, which is available in many commercial softwares such as EXCEL, MATLAB, etc.) is used to obtain a good solution. Good initial trial values are $\theta_B = \frac{\pi}{2}$ and $l = g$. The difference of springback calculations between using small gap and large gap assumptions will be discussed later in Section 4. It should be noticed that these relations depend on the given tooling set-up.

3.4 Springback calculation

In this analytical model, springback is considered to be a purely elastic recovery of the process. The springback angles of the straight part (θ_l) and the curved part (θ_s) are respectively derived. To derive the springback angle θ_l associated with the straight part l , one considers a free-body-diagram in Figure 5(a) assuming $M_A = 0$, $M_B = M_{elaspl}$, and the linear bending moment distribution along l being

$$M(s) = M_B \cdot \left(1 - \frac{s}{l}\right), \quad (33)$$

where $s \in [0, l]$. Differentiate Equation (33) to obtain

$$dM = -\frac{M_B}{l} ds. \quad (34)$$

Recall $d\theta = \kappa(s)ds$, or

$$\theta = \int_S \kappa(s) ds. \quad (35)$$

Apply these relations to the straight part l as follows

$$\theta_l = \int_0^s \kappa(s) ds, \quad (36)$$

$$\theta_l = \int_0^{M_B} \kappa(M) \left(\frac{l}{M_B} \right) dM. \quad (37)$$

Since springback is considered as the elastically-driven process, an elastic relationship between M and κ is recalled:

$$M = \frac{E \cdot t^3}{12} \kappa, \quad \text{or} \quad \kappa = \frac{12}{E \cdot t^3} M. \quad (38)$$

Substitute κ in Equation (38) into Equation (37)

$$\theta_l = \left(\frac{l}{M_B} \frac{12}{E \cdot t^3} \right) \int_0^{M_B} M dM = 6 \frac{l}{E \cdot t^3} M_B. \quad (39)$$

Therefore, the final expression for θ_l is written as follows

$$\theta_l = \frac{l}{t} \varepsilon_{y1} \gamma_B. \quad (40)$$

Similarly, to derive the springback angle θ_s associated with the curved part S , one considers a model in Figure 5(b) assuming the linear bending moment distribution along S as follows

$$M(s) = M_B + \frac{M_O - M_B}{S} s, \quad (41)$$

where $s \in [0, S]$. Similarly, one obtains

$$\theta_s = \left(\frac{S}{M_O - M_B} \frac{12}{E \cdot t^3} \right) \int_{M_B}^{M_O} M dM. \quad (42)$$

The final expression for θ_s is written as follows

$$\theta_s = \frac{S}{t} \varepsilon_{y1} \gamma_B (1 + M'). \quad (43)$$

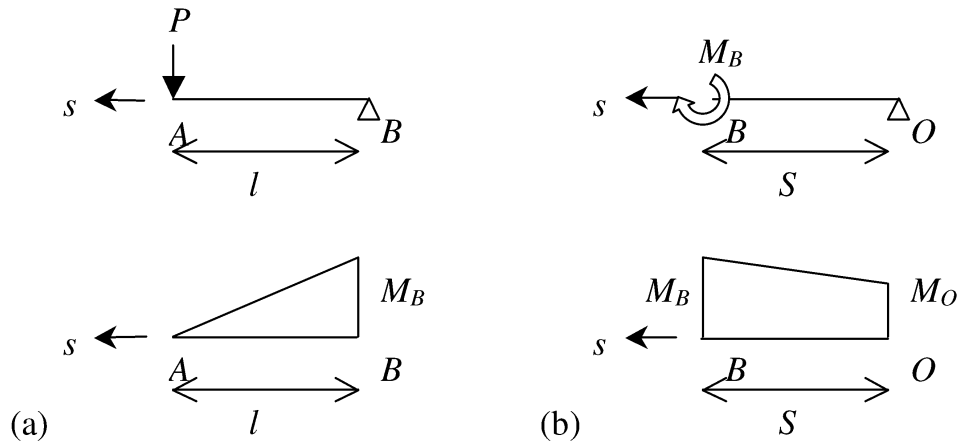
Both θ_l and θ_s are contributed and summed to the springback angle $\Delta\theta$ as follows

$$\Delta\theta = \theta_l + \theta_s. \quad (44)$$

The final configuration θ_f of the sheet is

$$\theta_f = \pi - \theta_P + \theta_l + \theta_s. \quad (45)$$

Figure 5 Free body diagrams and bending moment distributions of (a) the straight part and (b) the curved part



4 Comparisons with experimental results

To validate the proposed analytical model, the predicted results are compared with the corresponding experiments. Four materials (HS110, AKDQ, SAE980X, and a mild steel) are used, and the material data are summarised in Table 1. An approximation is used to transform the material data reported in [6] to the yield stress Y and the strength coefficient K as shown in Table 1.

Table 1 The summary of the material and tooling parameters

Material	E (GPa)	Y (MPa)	ν	K (MPa)	n	t (mm)	R (mm)
HS110	206.8	767.4	0.3	944.7	0.03714	0.79	3.18
AKDQ	206.8	$(206.8 + 159.3)/2$	0.3	614.2	0.22000	0.79	3.18
SAE980X	206.8	$(589.5 + 565.4)/2$	0.3	1091.0	0.13400	2.37	12.70
A mild steel	197.9	375.5	0.3	658.0	0.14000	1.55	20.00

For the proposed analytical model, both small gap and large gap assumptions are used and designated as ‘SG’ and ‘LG’, respectively. The predicted results are shown and compared in Figures 6–9.

Figure 6 The comparison between the predicted results from the analytical models and the experimental results from [7]

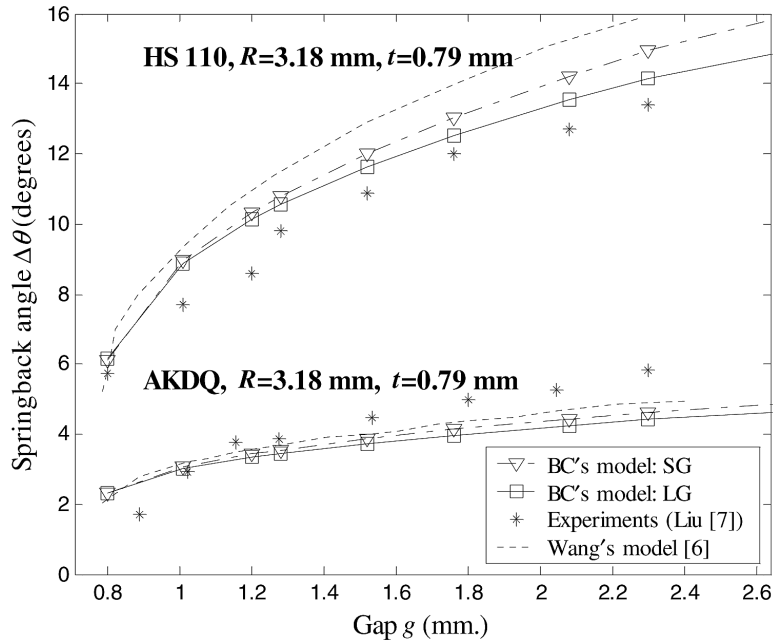


Figure 7 The comparison between the results from the analytical models and the experimental results from [8]

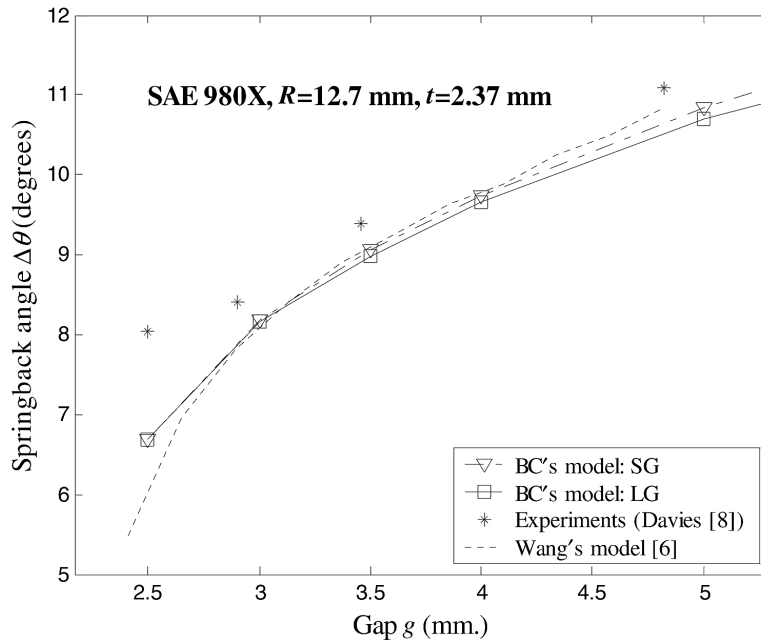


Figure 8 The effects of the gap and die corner radius on springback from the model

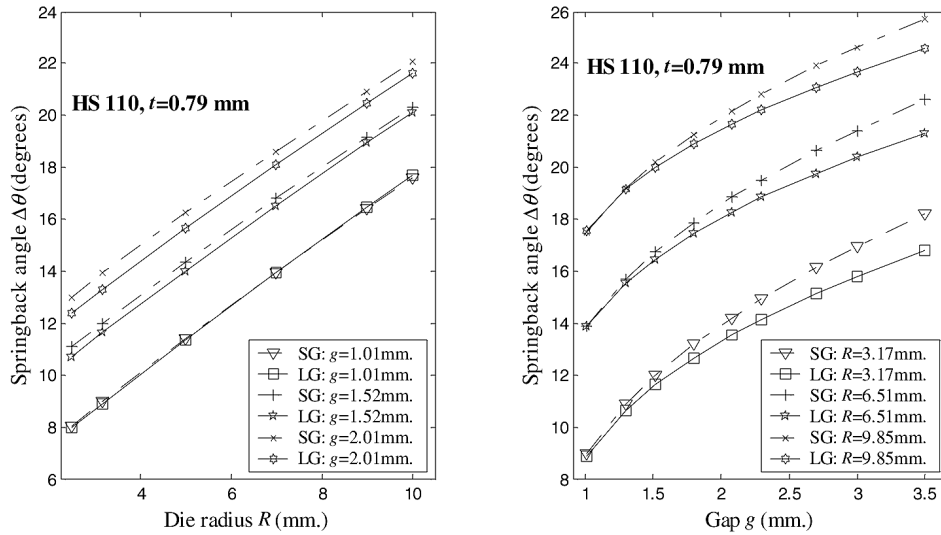
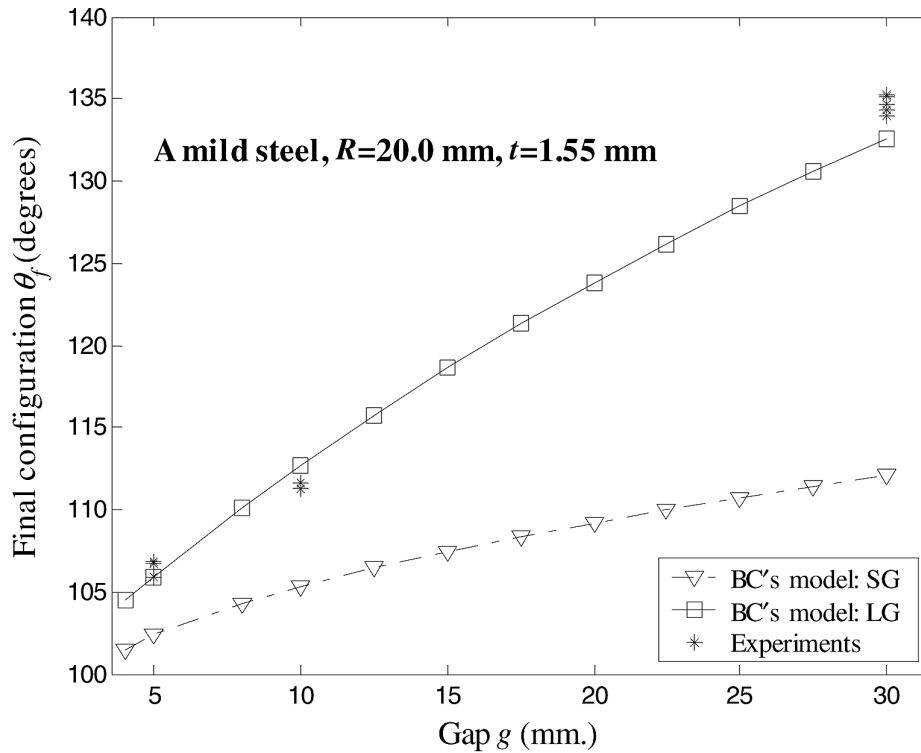


Figure 9 The comparison between the predicted results from the analytical model and the experimental results



In addition, the analytical model is used to observe the effects from the gap and the die corner radius as shown in Figure 8.

The analytical model is also verified with a large gap case. The mean or nominal values of the mild steel sheets shown in Table 1 (with $b_2 = -55.4216$ mm for the geometry relations shown in Appendix) are used to predict springback. Figure 9 shows the comparison between the predicted results from the analytical model and experimental results obtained at Advance Materials Processing Laboratory (AMPL) at Northwestern. Due to a different tooling set-up, the expressions for the geometry relations are presented in Appendix.

The predicted results from using the expansion of the true strain ε with the first-order term and that with higher-order terms are numerically computed to test the applicability of the analytical model. For the HS110 case, the springback angles $\Delta\theta$ at $g = 1.2$ mm are 10.265, 10.251, 10.252, and 10.252 degrees with the first-, second-, third- and fourth-order expansions, respectively. It can be seen that using the first-order of the series expansion of the true strain ε is effective.

5 Summary and concluding remarks

The analytical model for springback prediction for a straight flanging process has been proposed and summarised as follows:

$$E' = \frac{E}{1 - \nu^2}, \quad (46)$$

$$Y' = \frac{2Y}{\sqrt{3}}, \quad (47)$$

$$K' = \frac{2K}{\sqrt{3}}, \quad (48)$$

$$\varepsilon_{y1} = \frac{Y}{E}, \quad (49)$$

$$\kappa = \frac{1}{R} = \frac{1}{R_d + t/2}, \quad (50)$$

$$t_{y1} = \frac{1}{\kappa} \frac{Y}{E}, \quad (51)$$

$$t_{y2} = \frac{1}{\kappa} \left(\frac{Y}{K} \right)^{\frac{1}{n}}, \quad (52)$$

$$M_y = \frac{2}{3} Y \left(\frac{t}{2} \right)^2, \quad (53)$$

$$M_{elas} = \frac{2}{3} E \cdot \kappa \cdot (t_y)^3, \quad (54)$$

$$M_{plas1} = \text{MIN} \left[Y \cdot \left(\left(\frac{t}{2} \right)^2 - (t_{y1})^2 \right), \text{MAX} \left\{ Y \cdot \left((t_{y2})^2 - (t_{y1})^2 \right), 0 \right\} \right], \quad (55)$$

$$M_{plas2} = \text{MAX} \left[\frac{K}{n+2} \frac{2}{R^n} \left(\left(\frac{t}{2} \right)^{n+2} - t_{y2}^{n+2} \right), 0 \right], \quad (56)$$

$$M_B = M_{elasplas} = M_{elas} + M_{plas1} + M_{plas2}, \quad (57)$$

l and θ_B depend on the tooling set-up (see Section 3.3 for the expressions).

$$\gamma_B = \frac{M_B}{M_y}, \quad (58)$$

$$\theta_l = \frac{\varepsilon_{y1}}{t} \gamma_B l, \quad (59)$$

$$\theta_B = \theta_P - \theta_l, \quad (60)$$

$$M_O = P [l \cos(\theta_B - \theta_P) + R \sin(\theta_B - \theta_P)], \quad (61)$$

$$M' = \frac{M_O}{M_B}, \quad (62)$$

$$S = R \theta_B, \quad (63)$$

$$\theta_s = \frac{\varepsilon_{y1}}{t} \gamma_B S (1 + M'), \text{ and} \quad (64)$$

$$\Delta\theta = \theta_l + \theta_s. \quad (65)$$

Springback in the sheet metal forming process has been an important issue. To study springback, a number of experiments had been done while numerical simulations have been widely used due to the maturity of finite element methods. However, analytical models still play a role, especially in an early design stage, since they provide a quick estimation and also a qualitative understanding to designers.

It can be seen that the proposed analytical model is easy to implement and effective in predicting springback. The predicted results from the model show good agreements with the corresponding experiments at the different conditions used in Section 4. In addition, a comparison between the trends obtained from the analytical model and the experimental results in [5] shows good agreements, e.g. a lower gap causes lower springback, and a lower die radius causes lower springback. However, it should be noticed that variation and uncertainty of process parameters always exist in reality. Therefore, to draw a conclusion about the model validity, one may need to further perform an uncertainty analysis.

By analysing the results, it can be seen that changing the die corner radius has a greater effect than changing the gap. To use the small gap assumption, an observation from Figures 6–8 shows a disagreement between the predicted results from the two assumptions when the gap-and-thickness ratio is roughly larger than two. With the large gap assumption, the springback angle from the large gap assumption starts to level off, which reflects the reality. It is noted that the small gap assumption is a reduced form of the large gap assumption. Thus, they provide the same results at a small gap. The analytical model using only the first-order expansion of the true strain has shown its effectiveness of the prediction for general applications in Section 4 since the difference of the predictions using higher-order expansion is less than one percentage. The proposed analytical model shows flexibility and effectiveness in springback prediction for different tooling set-ups.

Acknowledgement

The support from NSF Grant (DMI-0084582) and Ford University Research Program is deeply appreciated.

References

- 1 Cao, J., Liu, Z. and Liu, W.K. (1999) 'On the structure aspect of springback in straight flanging', *Symposium on Advances in Sheet Metal Forming, 1999 ASME Winter Conference*.
- 2 Song, N., Qian, D., Cao, J., Liu, W.K. and Li, S. (2001) 'Effective prediction of springback in straight flanging', *Journal of Engineering Materials and Technology*, Vol. 123, No. 4, pp.456–461.
- 3 Muderrisoglu, A., Murata, M., Ahmetoglu, M.A., Kinzel, G. and Altan, T. (1996) 'Bending, flanging, and hemming of aluminum sheet: an experimental study', *Journal of Materials Processing Technology*, Vol. 59, pp.10–17.
- 4 Livatyali, H., Muderrisoglu, A., Ahmetoglu, M.A., Akgerman, N., Kinzel, G.L. and Altan, T. (2000) 'Improvement of hem quality by optimizing flanging and pre-hemming operations using computer aided die design', *Journal of Materials Processing Technology*, Vol. 98, pp.41–52.
- 5 Livatyali, H. and Altan, T. (2001) 'Prediction and elimination of springback in straight flanging using computer-aided design methods Part I: experimental investigations', *Journal of Materials Processing Technology*, Vol. 117, pp.262–268.
- 6 Wang, N.M. (1984) 'Predicting the effect of die gap of flange springback', *Proceedings of 13th Biennial IDDRG Congress*, Melbourne, Australia, pp.133–147.
- 7 Liu, Y.C. (1984) 'Springback reduction in U-channels: "double-bend" technique', *Journal of Applied Metalworking*, Vol. 3, No. 2, pp.148–156.
- 8 Davies, R.G. (1981) 'Springback in high-strength steels', *Journal of Applied Metalworking*, Vol. 1, No. 4, pp.45–52.
- 9 Hill, R. (1950) *The Mathematical Theory of Plasticity*, Oxford: Clarendon Press, p.355.
- 10 Wang, C.-T., Kinzel, G. and Altan, T. (1993) 'Mathematical modeling of plane-strain bending of sheet and plate', *Journal of Materials Processing Technology*, Vol. 39, pp.279–304.
- 11 Marciniak, Z., Duncan, J.L. and Hu, S.J. (2002) *Mechanics of Sheet Metal Forming*, Oxford: Butterworth-Heinemann, p.211.

Appendix

The true strain ε of the flanging process at an arbitrary local coordinate ζ is derived [10–11] as follows

$$\varepsilon = \ln \left[\frac{L}{L_0} \right] = \ln \left(\frac{Rd\theta + (R + \zeta)d\theta - Rd\theta}{Rd\theta} \right) = \ln(1 + \kappa\zeta). \quad (\text{A1})$$

The series expansion of Equation (A1) is

$$\ln(1 + \kappa\zeta) = \kappa\zeta - \frac{(\kappa\zeta)^2}{2} + \frac{(\kappa\zeta)^3}{3} - \frac{(\kappa\zeta)^4}{4} + \dots \text{ for } -1 < \kappa\zeta < 1. \quad (\text{A2})$$

Because $\kappa\zeta$ is usually a small number, the higher order terms of $\kappa\zeta$ can be neglected without losing accuracy. Therefore, the true strain expression can be written as

$$\varepsilon = \kappa\zeta. \quad (\text{A3})$$

Note that the expression in Equation (A2) is valid for this flanging application since $\kappa\zeta$ is always a set of $[-1, 1]$. One may also want to increase the numerical accuracy by adding higher-order terms, which can be numerically done.

For a large gap case with a small punch stroke pictured in Figure 1, we assume that the straight part (l) between points A and B is a straight line for the simplicity of explicit expressions. With the centre (a_1, b_1) of the die corner, the punch nose radius R_p , and the centre (a_2, b_2) of the punch nose, we derive a set of explicit expressions as follows.

$$l = \sqrt{u^2 + v^2}, \quad (\text{A4})$$

$$\theta_p = \arccos(xx), \quad (\text{A5})$$

where

$$u = \Delta a - RR \cdot yy,$$

$$v = \Delta b + RR \cdot xx,$$

$$xx = \left[\frac{\left(-\frac{\Delta b \cdot RR}{(\Delta a)^2} \right) + \left(1 + \frac{(\Delta b)^2}{(\Delta a)^2} - \frac{RR^2}{(\Delta a)^2} \right)^{0.5}}{\left(\frac{(\Delta a)^2 + (\Delta b)^2}{(\Delta a)^2} \right)} \right],$$

$$yy = \frac{\Delta b \cdot xx}{\Delta a} + \frac{RR}{\Delta a},$$

$$\Delta a = a_1 - a_2,$$

$$\Delta b = b_1 - b_2, \text{ and}$$

$$RR = (R_d + t) + R_p.$$